Check for updates

A dual pH- and reduction-responsive anticancer drug delivery system based on PEG–SS–poly(amino acid) block copolymer†

Bingqiang Li,[a] Meng Shan,[a] Xiang Di,[a] Chu Gong,[a] Lihua Zhang,[b] Yanming Wang[b] and Guolin Wu [ID] *[a]

A pH- and reduction-responsive anticancer drug delivery system was prepared and the triggerable and controllable drug release in response to stimuli was observed. In the first step, methoxy-poly(ethylene glycol) (mPEG) was conjugated with polysuccinimide (PSI) via disulfide linkages, and the PSI segment thereafter, was aminolyzed by 2-diisopropylaminoethylamine (DIPEA) and hydrazine hydrate (Hy). The obtained amphiphilic copolymer could form a bond with the model drug doxorubicin (DOX) at pH 7.4 via acid-labile hydrazone bonds, and more free DOX molecules could be encapsulated via hydrophobic interactions and $\pi-\pi$ stacking between the aromatic rings, leading to DOX-loaded micelles formation. These polymers and polymeric micelles then were characterized. The results showed that the polymeric micelles exhibited dual pH- and reduction-responsive disassembly behaviors. Moreover, while the blank copolymers had excellent cytocompatibility, the DOX-loaded micelles showed an enhanced drug release profile and improved cytotoxicity with decrease of pH and/or the addition of glutathione (GSH). These results indicated that the novel nanoparticle based on PEG–SS–poly(amino acid) block copolymer is a promising candidate for a carrier in controllable anti-tumor drug delivery.

1. Introduction

In the past few decades, more and more attention has been drawn to nano-sized drug or gene delivery systems, such as nanogels, nanoparticles and micelles,[1–13] due to their prolonged retention time, lower toxicity to normal cells, admirable biodegradability, and improved drug accumulation via the enhanced permeability and retention (EPR) effect.[14] Micelles, in particular, are widely utilized in research on anticancer drug nanocarriers due to their unique core–shell structures in which drugs are stably encapsulated in the 'core' and are difficult to be captured by the reticuloendothelial system (RES) undesirably during delivery to the targeted tumor site. Moreover, micelles are capable of releasing drugs in response to various internal and/or external stimuli such as temperature,[7] pH,[5,15,16] redox substances,[1,15,17,18] ultrasound,[19] and light;[20] thus increasing interests have been garnered with the in-depth study of the features of tumor microenvironment, e.g. decreased pH value, increased temperature and enriched reduction substances.[21,22]

[a]Key Laboratory of Functional Polymer Materials, Institute of Polymer Chemistry, College of Chemistry, Nankai University, Tianjin 300071, P. R. China. E-mail: guolinwu@nankai.edu.cn; Fax: +86 22 23502749; Tel: +86 22 23507746

[b]College of Pharmacy, Nankai University, Tianjin 300071, P. R. China

† Electronic supplementary information (ESI) available. See DOI: 10.1039/c7ra04254j

Among these stimuli-responsive drug delivery nanocarriers, pH-sensitive micelles have been widely exploited by numerous researchers since the extracellular pH value of solid tumors (pH 6.5–7.2) was verified to generally be lower than that of normal tissues (pH 7.4). In light of this finding, various polymers have been designed and their response to pH changes has been evaluated for controlled drug release applications. Wu et al.[11] developed a pH-responsive polymeric micelle based on poly(-ethylene glycol)-coupled poly(L-histidine) (PHIS–PEG$_{2000}$), in which significantly enhanced drug release was obtained when the pH value dropped from 7.4 to 5.0. Acid-labile chemical bonds or ionizable groups such as amino or imidazole[24] have been also introduced into polymers to design pH-responsive polymeric micelles.

Another kind of controlled drug release system that is of growing interest is the reduction-responsive micelle. Gluta-thione (GSH) as a reductive substance exists not only in cyto-plasm but also in extracellular microenvironment, and it has been discovered that the intracellular compartments tend to contain more concentrated GSH than extracellular environments. The intracellular concentration of GSH is approximately 10–1000 folds higher than that of extracellular.[23,24] Interestingly, disulfide bonds can be easily cleaved when they encounter with concentrated GSH in cells while they are relatively stable in extracellular environments. In view of this, some drug delivery systems which can respond to abundant GSH in cells have been prepared. Chen's research group[12] developed a biocompatible

reduction-responsive micellar system by synthesizing disulfide-linked block copolymers (mPEG–S$_2$–PZLL), and doxorubicin (DOX)-loaded micelles showed accelerated drug release triggered by 10.0 mM GSH.

In practice, micelles are constructed using amphiphilic copolymers in which polyethylene glycol (PEG) were often used to serve as the hydrophilic segment because of its excellent biocompatibility and non-immunogenic property.[25] Moreover, poly(aspartic acid) derivatives with hydrophobic grafts are commonly used as the hydrophobic moiety due to their attractive biodegradability and biocompatibility.[26] Herein we presented a dual pH- and reduction-responsive drug delivery system that was prepared by conjugating PEG with polysuccinimide (PSI) using disulfide as the linker and the PSI moiety, thereafter was furnished with 2-diisopropylaminoethylamine (DIPEA) and hydrazine hydrate (Hy) respectively *via* ring opening reactions; and finally, doxorubicin (DOX) was bonded to the backbone chemically *via* acid-labile hydrazone bonds and more DOX molecules were physically encapsulated *via* hydrophobic interactions and π–π stacking during the self-assembly process at pH 7.4. The ^{1}H NMR, Fourier transform infrared spectroscopy (FT-IR), zeta potential, dynamic laser scattering (DLS), and transmission electron microscopy (TEM) measurements were performed to characterize the materials. The DOX-loaded micelles exhibited a pH- and reduction-dependent drug release profile. The excellent cytocompatibility of polymers and the cytotoxicity of DOX-loaded micelles indicated that the novel conjugate was a promising anti-tumor drug delivery system.

2. Experiment

2.1. Materials

Monoethoxy poly(ethylene glycol) (mPEG) (M_n = 20 000 Da) and 2,2-dithiodiethanol (DiT) were purchased from Sigma-Aldrich. L-Aspartic acid (L-Asp) and *N,N*-diisopropylaminoethylamine (DIPEA) were obtained from Aladdin Reagent Company. *N,N'*-Carbonyldiimidazole (CDI) and doxorubicin hydrochloride (DOX·HCl) were supplied by Heowns Biochem Technologies Co. Ltd. L-Buthionine-sulfoximine (BSO) was purchased from Shanghai Yuanye Biological Technology Co. Ltd. Hydrazine hydrate (80%) and other reagents were purchased from Tianjin Chemical Reagent. All the reagents were used without further purification.

2.2. Synthesis of disulfide-functionalized monoethoxy poly(ethylene glycol) (mPEG–SS–OH)

The mPEG–SS–OH was synthesized according to the method reported previously.[27] In brief, mPEG and CDI solutions were prepared by dissolving 4.0 g (0.2 mmol) of mPEG and 0.162 g (1.0 mmol) of CDI powder in 20 and 5 mL of *N,N*-dimethylformamide (DMF), respectively. The mPEG solution was added dropwise to the CDI solution and the mixture was stirred at room temperature for 24 h. Then, the prepared mixture was added dropwise to DiT solution (prepared by dissolving 0.26 g DiT (1.5 mmol) in 5 mL DMF), and the new mixture was stirred at room temperature for another 12 h. The resulting solution

was then placed in a dialysis bag with molecular weight cut off (MWCO) of ~3500 Da and dialyzed against distilled water. Finally, the cotton-shaped mPEG–SS–OH solid was obtained by lyophilization.

2.3. Synthesis of monoethoxy poly(ethylene glycol)–polysuccinimide conjugate with disulfide linkages (mPEG–SS–PSI)

The solid mPEG–SS–OH (0.76 g, 0.038 mmol) was dissolved in 7 mL of DMF, while 0.081 g (0.5 mmol) of CDI was dissolved in 3 mL of DMF. Thereafter the mPEG–SS–OH solution was dropwise added to the CDI solution, and the mixture was stirred at room temperature for 24 h. The obtained mixture was then dropwise added to PSI (10.8 g) dissolved in DMF (40 mL), and the new mixture was stirred at room temperature for another 30 h. The PSI was synthesized according to Kang *et al.*[28] To remove excess reactants and other by-products, the resulting solution was first dialyzed against dimethylsulfoxide (DMSO), followed by distilled water in a dialysis bag (MWCO = 25 000 Da). The cotton-shaped mPEG–SS–PSI solid was obtained by lyophilization, in the final step.

2.4. Synthesis of DIPEA and hydrazide modified mPEG–SS–PSI (mPEG–SS–PDPH)

The mPEG–SS–PSI (0.5 g) and DIPEA (0.65 g, 4.5 mmol) were mixed and dissolved in 5 mL of DMF. The reaction mixture was then stirred at 50 °C under argon atmosphere for 10 h. After the solution was cooled down to room temperature, 1.0 g (25 mmol) of hydrazine hydrate was added to the solution, which was then stirred at 25 °C under argon atmosphere for 8 h. Thereafter, the final product mPEG–SS–PDPH solid was obtained by the method described for the mPEG–SS–PSI.

2.5. DOX-loaded micelles preparation

The mPEG–SS–PDPH (0.1 g) and DOX·HCl (0.02 g) were mixed and dissolved in 20 mL of DMSO, and stirred in the dark for 24 h. Thereafter, triethylamine (10.5 mg) was slowly added to the solution, and the resulting mixture was further stirred in the dark for another 12 h. Afterwards, distilled water (40 mL) was added to the mixture using a constant flow pump, and the mixture continued to stir in the dark for additional 12 h. Finally, the resulting solution was dialyzed against 10 mM PBS (pH 7.4) in the dark using a dialysis tube membrane (MWCO = 3500 Da) for 48 h, and then subjected to lyophilization to yield the solid DOX-loaded micelles (mPEG–SS–PAPH-hyd-DOX). The drug loading content (%) and entrapment efficiency (%) were calculated as shown below:

$$\text{Loading content } (\%) = \frac{\text{mass of loaded DOX}}{\text{mass of nanoparticles}} \times 100\%$$

$$\text{Entrapment efficiency } (\%) = \frac{\text{final loaded DOX}}{\text{initial feed DOX}} \times 100\%$$

2.6. Measurements

2.6.1 Nuclear magnetic resonance (NMR) characterization. ^1H NMR spectra were recorded on a UNITY-plus 400 NMR spectrometer (Varian, Switzerland) using DMSO-d_6 as the solvent.

2.6.2 Fourier transformed infrared (FT-IR) characterization. Fourier transform infrared (FT-IR) spectra were obtained on a FTS6000 spectrophotometer (Bio-Rad, America) using KBr powder as control. 64 scans in all were performed from 400 cm^{-1} to 4000 cm^{-1} at a resolution ratio of 4 cm^{-1}.

2.6.3 Gel permeation chromatography (GPC). Absolute molecular weights and molecular weight distributions of PSI and mPEG–SS–PSI were determined by GPC (Viscotek GPC270 system, Malvern Instruments), with a light scattering detector. The column was silica column. DMF was used as eluent at a flow rate of 1.0 mL min^{-1}.

2.6.4 Dynamic light scattering (DLS) and zeta potential (ZP) measurements. The hydrodynamic diameters of the nanoparticles were analyzed by DLS using a Zetasizer Nano ZS90 (Malvern Instruments, UK). The measurements were conducted at 25 $^\circ$C at a scattering angle of 90°. The zeta potential of mPEG–SS–PDPH was also recorded using Zetasizer Nano ZS90. Three repeated measurements were performed for each sample.

2.6.5 Transmission electron microscopy (TEM). The morphology of nanoparticles was observed by TEM. The images were recorded by using a JEM2100EX microscope (JEOL Ltd, Japan). Samples were prepared *via* the following method: a drop of the micelle solution was dropped onto a carbon-coated copper grid and then dried by means of vacuum drying for 24 h.

2.6.6 Ultraviolet-visible (UV-vis) spectroscopy. UV-vis spectroscopic measurements were carried out on a UV-2450 spectrophotometer (Shimadzu Co., Japan).

2.6.7 *In vitro* drug release experiment. Firstly, 8 mg of the DOX-loaded polymeric micelles were dispersed in 2 mL of PBS (pH 7.4). The solution was then sealed in dialysis membrane (MWCO = 3500 Da) and immersed in tubes containing 18 mL of varying buffer: pH 7.4 with and without 10 mM GSH, and pH 5.0 with and without 10 mM GSH. The tubes were then shaken on a shaking bed at 37 $^\circ$C. At each defined time interval, 3 mL of the release media was sampled and replaced with 3 mL of the corresponding buffer. The DOX concentration was determined by a UV-vis spectrophotometer at 495 nm wavelength. Cumulative release of DOX (%) was calculated according to the following formula:

$$\text{Cumulative release of DOX } (\%) = \frac{V_e \sum_1^{n-1} C_i + V_0 C_n}{m_0} \times 100\%$$

where V_e is the volume of release media removed every time (3 mL), V_0 is the total volume of release media (18 mL), C_i is the concentration of DOX in the release media, and m_0 is the total mass of DOX entrapped in micelles.

2.6.8 *In vitro* cell cytotoxicity tests. The cytotoxicity of mPEG–SS–PDPH copolymers was evaluated in A549 cells (adenocarcinomic human alveolar basal epithelial cells) by an MTT assay. In brief, the cells were seeded in DMEM complete medium in 96-well plates at a density of 1×10^4 cells per well and cultured at 37 $^\circ$C with 5% CO_2 for 24 h. After that, the mPEG–SS–PDPH polymer solutions at varying concentrations (0, 5, 10, 50, 100, 250, 500 µg mL^{-1}) were added to the corresponding wells and the cells were further incubated at the same condition for 48 h. The cells were then subjected to the MTT assay. The medium in each well was first replaced with MTT dye (100 µL, 0.5 mg mL^{-1} in PBS) and incubated for 4 h. Thereafter, the medium was removed and 150 µL of DMSO was added to each well. The resulting cell solutions were measured for their absorbance at a wavelength of 570 nm by using a microplate reader (Labsystem, Multiskan, Ascent, Model 354 Finland). The percentage of cell viability was calculated in contrast to the negative control (PBS). Each sample (*i.e.* each different concentration of the mPEG–SS–PDPH polymer solution) was done in six replicates and mean values were calculated and presented in the final data. The A549 cells were supplied by the Institute of Radiation Medicine, Chinese Academy of Medical Sciences.

The MTT assay was also performed to study the cytotoxicity of free DOX and DOX-loaded micelles to A549 cells under varying conditions: pH 7.4, pH 6.0, and pH 7.4 with 0.11 mg mL^{-1} BSO (a specific inhibitor of the glutathione synthesis pathway in cells, which can decrease concentration of GSH in A549 cells). The method, number of replicates, and calculation were the same as that of the mPEG–SS–PDPH polymer. However, the mPEG–SS–PDPH polymer solutions were replaced by free DOX or DOX-loaded micelles. In addition, for the condition at pH of 7.4 with BSO, cells were pre-incubated with 0.11 mg mL^{-1} BSO for 12 h prior to adding DOX-loaded micelles, which were then further incubated for 24 h.

3. Results and discussion

3.1. Synthesis and characterizations of the polymers

Scheme 1 illustrates the synthesis route for the preparation of mPEG–SS–PDPH used in the pH- and reduction-responsive drug
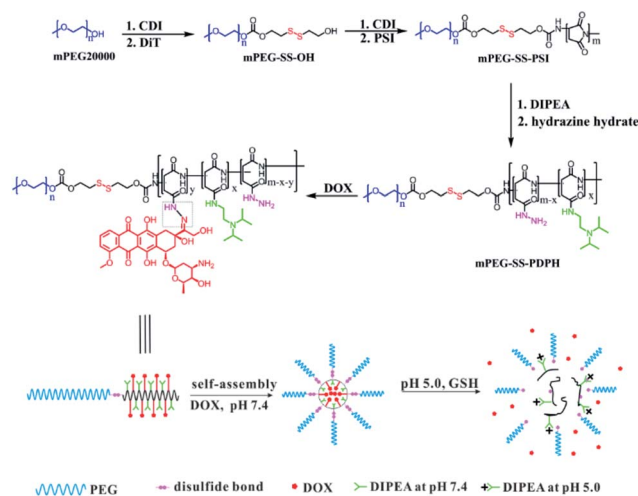
Scheme 1 The synthesis route of mPEG–SS–PDPH, and the suggested DOX encapsulation and pH- and reduction-dependent release process.

delivery system and the suggested DOX encapsulation and pH- and redox-dependent release processes. The mPEG–SS–OH was functionalized with disulfide bonds by conjugating mPEG$_{20000}$ with DiT using CDI as the linker. Thereafter, the mPEG–SS–OH was coupled with PSI in order to prepare mPEG–SS–PSI using the same linker (CDI). The copolymer mPEG–SS–PDPH was then synthesized by the successive aminolysis reactions of the PSI segment in mPEG–SS–PSI. Finally, DOX was chemically bound to or physically encapsulated into the core of the micelles *via* hydrazone bonds or hydrophobic interactions and π–π stacking. In addition, the mechanism of the reactions is shown in ESI Fig. S2.†

The ^{1}H NMR spectra of the prepared polymers are shown in Fig. 1. The presence of the peaks at 4.19 and 4.13 ppm in Fig. 1(B) indicated that mPEG$_{20000}$ and DiT were successfully conjugated. The ratio of the integral area of d and e was calculated to be 1 : 0.939, indicating that the conversion ratio from mPEG$_{20000}$ to mPEG–SS–OH was 93.9%. The absence of peak g in Fig. 1(C) as well as the presence of peaks j, k, and k′, the decrease and increase of the integral area of peaks at 3.65 and 3.8 ppm, respectively in Fig. 1(C) indicated the successful preparation of the mPEG–SS–PSI. Furthermore, peak a and j were used to calculate the block ratio in mPEG–SS–PSI. The result demonstrated that 98.7% of mPEG–SS–OH was converted to mPEG–SS–PSI. Additionally, in Fig. 2, the presence of peaks d, e and g indicated that the DIPEA is grafted to the backbone of the PSI segment, while the absence of the 5.3 ppm peak and the presence of 4.5 ppm peak indicated that the PSI moiety of mPEG–SS–PSI was completely ring-opened by DIPEA and Hy. Finally, by comparing the integral area of peak g and b in Fig. 2, the grafting ratio of DIPEA and Hy was calculated to be 57.5%
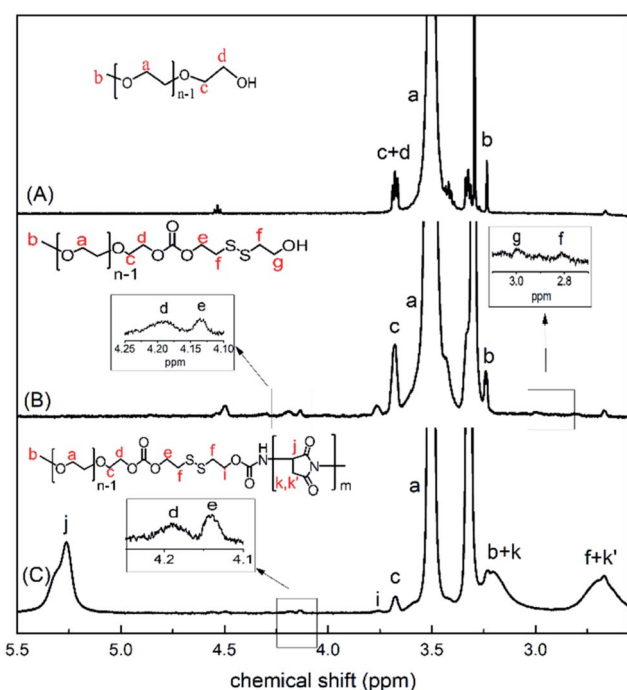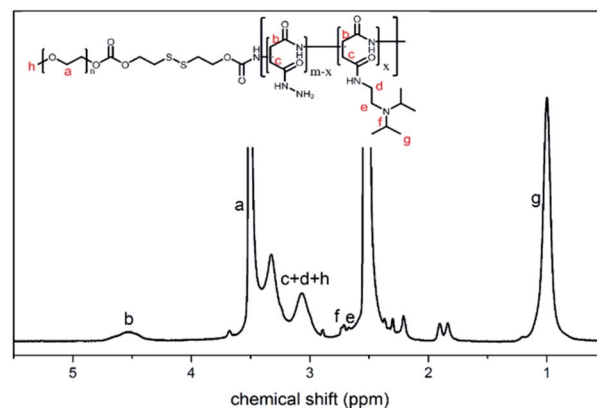

Fig. 2 ^{1}H NMR spectrum of mPEG–SS–PDPH in DMSO-d$_6$.

and 42.5%, respectively. The M_n of mPEG–SS–PDPH is calculated to be about 56 kDa.

Fig. 3 shows the FT-IR spectra of PSI, mPEG$_{20000}$, mPEG–SS–OH, mPEG–SS–PSI and mPEG–SS–PDPH. Compared with the spectrum of mPEG$_{20000}$ in Fig. 3(B), a band at 1755 cm^{-1}, which belonged to the vibration absorptions of carbonyl groups in mPEG–SS–OH, were observed in Fig. 3(E), suggesting that the mPEG–SS–OH was successfully prepared. Bands at 2881 and 1105 cm^{-1} in Fig. 3(E) were assigned to the vibration absorptions of C–H and C–O bonds of mPEG–SS–OH, whereas bands at 1798 and 1717 cm^{-1} in Fig. 3(A) were attributed to the imide rings of PSI. In addition, the presence of absorption bands at 2881, 1105, 1798, and 1717 cm^{-1} in Fig. 3(C) indicated the existence of PEG and PSI blocks in mPEG–SS–PSI. In Fig. 3(D), the absence of the bands at 1798 and 1717 cm^{-1} confirmed the complete ring opening reaction of PSI moiety. Moreover, bands at 1650, 1540, and 3300 cm^{-1} in Fig. 3(D) were the typical absorption bands of the corresponding amide I, amide II, and N–H bonds in mPEG–SS–PDPH structure. These results confirmed the successful preparation of mPEG–SS–PDPH and other polymers. In addition, the FT-IR spectra of mPEG–SS–
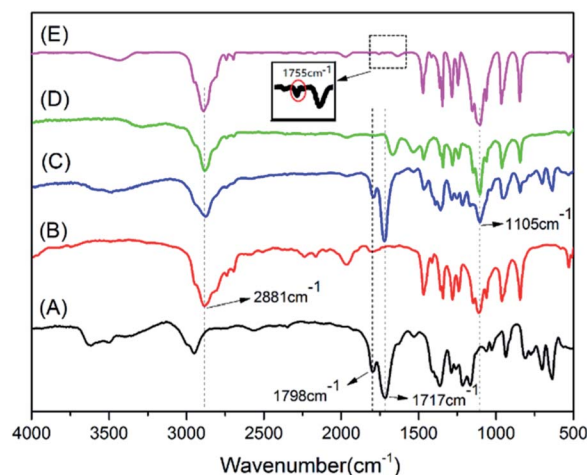

Fig. 1 ^{1}H NMR spectra of mPEG$_{20000}$ (A), mPEG–SS–OH (B) and mPEG–SS–PSI (C) in DMSO-d$_6$.

Fig. 3 FT-IR spectra of PSI (A), mPEG$_{20000}$ (B), mPEG–SS–PSI (C), mPEG–SS–PDPH (D) and mPEG–SS–OH (E).

PDPH-hyd-DOX and mPEG–SS–PDPH are shown in ESI Fig. S3.†
The peak at 1615 cm^{-1} in the FT-IR spectrum of mPEG–SS–
PDPH-hyd-DOX, corresponding to the stretching vibration of
C=N in the hydrazone bonds, suggested a successful conjuga-
tion of DOX and mPEG–SS–PDPH. Finally, GPC was performed
to obtain the molecular weight (M_n) of PSI and mPEG–SS–PSI,
which were found to be 18 000 (PDI = 1.7) and 35 600 (PDI =
1.9), respectively; and considering the M_n of mPEG are 20 000
Da, the conjugate block copolymer mPEG–SS–PSI was synthe-
sized successfully. The GPC curve of mPEG–SS–PSI was shown
in the ESI Fig. S1.†

3.2. DOX-loaded micelles preparation

The DOX-loaded polymeric micelles (mPEG–SS–PDPH-hyd-
DOX) were prepared by the reaction between mPEG–SS–PDPH
and DOX, resulting in chemical bonds between mPEG–SS–
PDPH and DOX, as well as the π–π stacking between the
bonded DOX and the free DOX. Fig. 4 shows the hydrodynamic
diameter and TEM image of the micelles formed by mPEG–SS–
PDPH-hyd-DOX at pH 7.4. The hydrodynamic diameter deter-
mined by DLS was 161 nm with PDI of 0.22. In contrast, the
diameter measured from TEM was approximately 120 nm,
smaller than that from DLS measurement, which is the result of
dehydration of the micelles during sample preparation for TEM
imaging. The TEM image, however, showed that mPEG–SS–
PDPH-hyd-DOX could self-assemble into near spherical
micelles. According to the UV-vis measurements, the loading
content and encapsulation efficiency were measured to be 9.4%
and 51.8%, respectively.

3.3. pH-Responsive behavior

It is known that polymers with diisopropylaminoethyl groups
are pH-responsive[29,30] because the tertiary amine group can be
more protonated upon decreasing pH so that the polymers
become more hydrophilic. Moreover, a portion of DOX payload
is attached to the backbone of the polymer *via* an acid-labile
hydrazone bond, thus the chemically linked DOX is released
when the pH value drops to 6.5 (the pH value of extracellular
microenvironment of cancer cells) or even lower (the pH value
in endosomes or lysosomes). Thus, diisopropylaminoethyl
groups and hydrazone bonds were introduced into the poly-
meric DOX-loaded micelles and the drug release triggered by
changes of pH were studied. Fig. 5 shows that the zeta potential
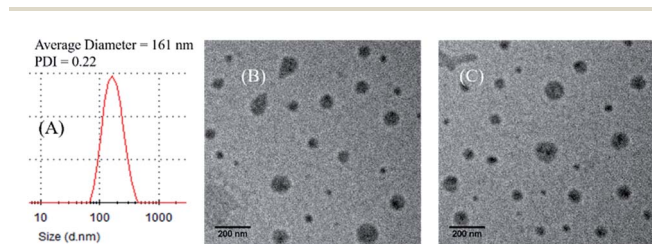(ZP) of mPEG–SS–PDPH descended from 15 to −8 mV when pH

Fig. 5 Relationship of pH and zeta potential of mPEG–SS–PDPH in
aqueous solution (1 mg mL^{-1}). Data are shown as mean ± SD (n = 3).

values increased from 4 to 10; and the ZP became 0 when the pH
value is about 9.2.

Furthermore, changes of DOX-loaded micelle diameters at
pH 5.0 were observed by TEM images. The results shown in
Fig. 6, demonstrated that the diameter of the micelles increased
from ∼120 nm (Fig. 6(A)) to ∼220 nm (Fig. 6(B)) in the first 0.5 h,
and then further increased to ∼403 nm upon disassembly of the
micelles, which finally led to DOX release after 3 h (Fig. 6(D)).
The data demonstrated that the DOX-loaded micelles we pH-
responsive and the drug release could be triggered by
lowering pH value.

3.4. Morphology and reduction-responsive behavior

Fig. 7 exhibits the morphology of DOX-loaded micelles after
being treated by 10 mM GSH for varying time. The results
demonstrated that micelle diameters increased from ∼120 nm
(Fig. 7(A)) to ∼180 nm (Fig. 7(B)), and eventually increased to
∼200 nm (Fig. 7(C)). The changes of the diameters may be due

Fig. 4 The hydrodynamic diameter (A) and TEM image of micelles
constructed by PEG–SS–PDPH-hyd-DOX at pH 7.4 after vibration for
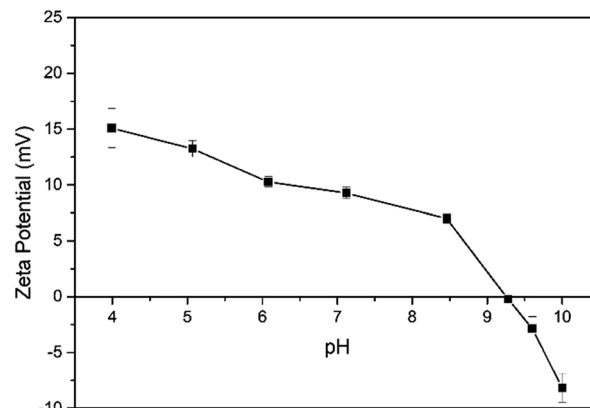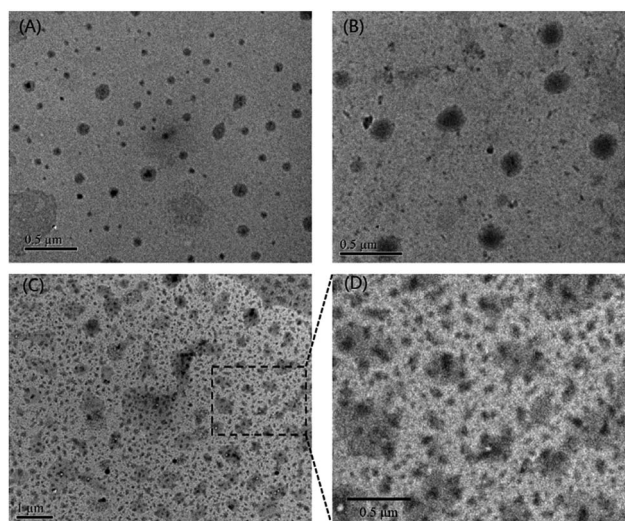0 h (B) and 3 h (C).

Fig. 6 TEM images of mPEG–SS–PDPH-hyd-DOX micelles at pH 5.0
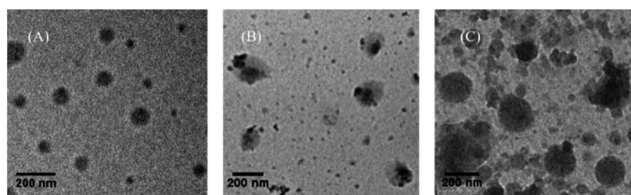without GSH for 0 h (A), 0.5 h (B) and 3 h (C and D).

Fig. 7   TEM images of mPEG–SS–PDPH-hyd-DOX micelles at pH 7.4 with GSH (10 mM) at 0 h (A), 0.5 h (B) and 3 h (C).

to that the micelles shed their PEG shells in a reductive environment so that the hydrophobic core could form larger and irregular aggregates. Thus, these results confirmed the reduction-responsiveness of the micelles.

3.5. *In vitro* drug release

In vitro drug release measurements were performed under different conditions including: pH 7.4 with and without 10 mM GSH, and pH 5.0 with and without 10 mM GSH, and the results are shown in Fig. 8. Approximately 5% of the drug payload was released from the DOX-loaded micelles within 130 h at pH 7.4 without GSH, indicating that the micelles will be stable with very little DOX leakage in a normal physiological environment. According to the release profile at pH 5.0 without GSH, drug release rate was higher than that at pH 7.4 without GSH, and the rate gradually decreased after the burst release during the initial several hours. The ultima drug release ratio of DOX-loaded micelles at pH 5.0 without GSH was about 28%, which is much higher than that at pH 7.4 without GSH. This is because the acid-sensitive hydrazone bond between the backbone of the polymer and the chemically-linked DOX was hydrolyzed when the pH value descended from 7.4 to 5.0. In addition, it is possible that the tertiary amine group was apt to be protonized at pH 5.0 to make the core of the micelle more hydrophilic, leading to swelling of micelles and drug release. The results
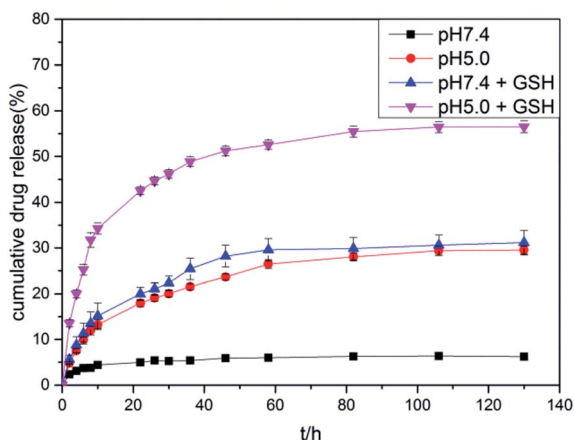
indicated that the DOX-loaded micelles showed a pH-dependent drug release profile.

Although the release profile of DOX-loaded micelles at pH 7.4 with 10 mM GSH was similar to that at pH 7.4 without GSH, the final cumulative drug release ratio was about 31% within 130 h, which was significantly higher. The reason for this could be that GSH could reduce and break the disulfide bonds between the PEG shells and the cores, causing DOX to be released from the core of micelles by the deshielding effect. Thus this result further verified the reduction-responsive property of DOX-loaded micelles. Nevertheless a very small amount of mPEG-PSI might exist in the product (<7% in this system). However, based on *in vitro* drug release, a small amount of mPEG-PSI will not affect the reduction-responsiveness of this system.

As a combination of pH- and reduction-responsiveness, the cumulative drug release percentage of DOX-loaded micelles at pH 5.0 with 10 mM GSH was higher than that at pH 5.0 without GSH or at pH 7.4 with 10 mM GSH. The final release ratio is about 58% and a more effective and sustained release was observed. These results thus demonstrated that the novel DOX-loaded micelles could potentially be utilized as controlled drug delivery systems.

3.6. Kinetics of drug release

The Korsmeyer–Peppas semi-empirical equation was used to investigate the drug release mechanism:

$$Q_t/Q_e = k_{KP}t^n$$

Q_t/Q_e represents the fraction of drug released at time t, k_{KP} is the constant related to the structural and geometric characteristics of the micelles, and n is the release exponent, an indicator of drug release mechanism. According to the data from the first several hours of drug release, the kinetic exponents (n) at pH 7.4 without GSH, pH 5.0 without GSH, pH 7.4 with 10 mM GSH, pH 5.0 with 10 mM GSH were found to be 0.36, 0.64, 0.62 and 0.59, respectively. All correlation coefficients (R^2) obtained were higher than 0.99. The results indicated that the kinetics of drug release at pH 7.4 without GSH agreed with a typical Fickian diffusion, while random diffusion controlled release kinetics, resulting from the molecular chain movement combined with the Fickian diffusion was observed for other three conditions (pH 5.0 with and without 10 mM GSH, and pH 7.4 with 10 mM GSH). This may be because under these three conditions the micelles shed their PEG shells by breakage of disulfide bonds and/or the tertiary amine was ionized and hydrazine bond was broken at a low pH, which led to destruction of the micelles. Finally, the forces of Fickian diffusion and random diffusion were combined to control the pH- and reduction-dependent drug release.

3.7. *In vitro* cytotoxicity

Cytocompatibility of the copolymer was evaluated using the MTT assay in A549 cells at pH 7.4 at 37 °C. As shown in Fig. 9(A), the copolymer mPEG–SS–PDPH at varying concentrations from

Fig. 8   Time dependent cumulative release profiles of DOX from PEG–SS–PDPH-hyd-DOX nanoparticles at varying conditions. Data are shown as mean ± SD ($n = 3$).
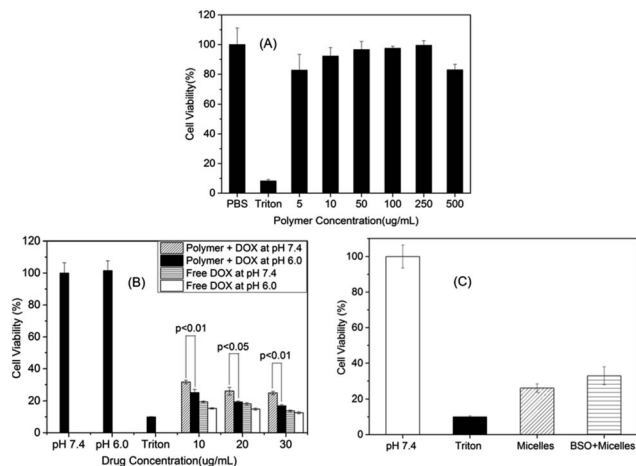
Fig. 9 (A) *In vitro* cytotoxicity of mPEG–SS–PDPH at various concentrations to A549 cells. (B) *In vitro* cytotoxicity of DOX-loaded micelles and free DOX against A549 cells at pH 7.4 without GSH and pH 6.0 without GSH at 37 °C. (C) *In vitro* cytotoxicity of DOX-loaded micelles (20 μg mL^{-1}) against A549 cells at pH 7.4 with BSO (0.11 mg mL^{-1}) or without BSO at 37 °C.

5 to 500 μg mL^{-1} was of low cytotoxicity with a cell viability of more than 80% after 48 h incubation, indicating that the copolymer mPEG–SS–PDPH possessed excellent cytocompatibility.

The cytotoxicity of the DOX-loaded micelles to A549 cells at various conditions (pH 7.4, pH 6.0 and pH 7.4 with 0.11 mg mL^{-1} BSO) was also evaluated using the same assay. Fig. 9(B) shows the cytotoxicity of free DOX and DOX-loaded polymeric micelles to A549 cells at pH 7.4 or pH 6.0, and this indicated that the DOX-loaded micelles at pH 6.0 were more cytotoxic to A549 cells than those at pH 7.4 due to the more drug release triggered by the protonation of tertiary amine groups and the hydrolysis of hydrazone bonds at a lower pH value. The cytotoxicity of DOX-loaded polymeric micelles to A549 cells at pH 7.4 with or without 0.11 mg mL^{-1} BSO is shown in Fig. 9(C). The result demonstrated that the cell viability at pH 7.4 with BSO was lower than that at the same pH without BSO, which could be explained in that BSO, as an inhibitor of GSH synthesis, could reduce GSH concentration in cells, causing inability of the micelles to shed their PEG shells, resulting in less DOX release and thus higher cell viability. On the other hand, in A549 cells without BSO treatment, their intracellular GSH was not inhibited and was able to break disulfide bonds to accelerate the drug release, leading to more cell death. The *in vitro* cytotoxicity tests indicated that the DOX-loaded micelles could release drugs in response to changes of pH or GSH concentration, therefore, are promising drug carriers for controlled drug release and cancer therapy.

4. Conclusions

In this work, a dual pH- and reduction-responsive anticancer drug delivery system was developed by conjugating mPEG and PSI using a disulfide linker, followed by the modifications of PSI

via ring opening reactions with 2-diisopropylaminoethylamine and hydrazine hydrate. DOX was chemically or physically encapsulated in the self-assembled polymeric micelles in PBS. The blank copolymer showed excellent cytocompatibility while the DOX-loaded micelles exhibited enhanced cytotoxicity against cancer cells at low pH or in the presence of GSH. In conclusion, the DOX-loaded micelles could potentially be used as anti-tumor drug delivery systems with a controllable release manner in cancer therapy.

Acknowledgements

References

1 C. Y. Ang, S. Y. Tan, C. Teh, J. M. Lee, M. F. E. Wong, Q. Qu, L. Q. Poh, M. Li, Y. Zhang, V. Korzh and Y. Zhao, *Small*, 2017, **13**, 1602379.

2 P. Zhang, H. Zhang, W. He, D. Zhao, A. Song and Y. Luan, *Biomacromolecules*, 2016, **17**, 1621–1632.

3 C. Wu, J. Yang, X. Xu, C. Gao, S. Lü and M. Liu, *Eur. Polym. J.*, 2016, **83**, 230–243.

4 N. Kamaly, B. Yameen, J. Wu and O. C. Farokhzad, *Chem. Rev.*, 2016, **116**, 2602–2663.

5 H. Yu, J. Sun, Y. Zhang, G. Zhang, Y. Chu, R. Zhuo and X. Jiang, *J. Polym. Sci., Part A: Polym. Chem.*, 2015, **53**, 1387–1395.

6 S. Lv, Z. Tang, D. Zhang, W. Song, M. Li, J. Lin, H. Liu and X. Chen, *J. Controlled Release*, 2014, **194**, 220–227.

7 R. Li, F. Feng, Y. Wang, X. Yang, X. Yang and V. C. Yang, *J. Colloid Interface Sci.*, 2014, **429**, 34–44.

8 Y. Chu, H. Yu, Y. Ma, Y. Zhang, W. Chen, G. Zhang, H. Wei, X. Zhang, R. Zhuo and X. Jiang, *J. Polym. Sci., Part A: Polym. Chem.*, 2014, **52**, 1771–1780.

9 M. Cai, K. Zhu, Y. Qiu, X. Liu, Y. Chen and X. Luo, *Colloids Surf., B*, 2014, **116**, 424–431.

10 J. Yu, X. Li, Y. Luo, W. Lu, J. Huang and S. Liu, *Colloids Surf., B*, 2013, **107**, 213–219.

11 H. Wu, L. Zhu and V. P. Torchilin, *Biomaterials*, 2013, **34**, 1213–1222.

12 J. Ding, J. Chen, D. Li, C. Xiao, J. Zhang, C. He, X. Zhuang and X. Chen, *J. Mater. Chem. B*, 2013, **1**, 69–81.

13 M. Kumagai, Y. Imai, T. Nakamura, Y. Yamasaki, M. Sekino, S. Ueno, K. Hanaoka, K. Kikuchi, T. Nagano, E. Kaneko, K. Shimokado and K. Kataoka, *Colloids Surf., B*, 2007, **56**, 174–181.

14 N. Ohtsuka, T. Konno, Y. Miyauchi and H. Maeda, *Cancer*, 1987, **59**, 1560–1565.

15 W. Chen, P. Zhong, F. Meng, R. Cheng, C. Deng, J. Feijen and Z. Zhong, *J. Controlled Release*, 2013, **169**, 171–179.

16 P. Vaupel, F. Kallinowski and P. Okunieff, *Cancer Res.*, 1989, **49**, 6449–6465.

17 X. Hu, Y. Wang, L. Zhang, M. Xu, W. Dong and J. Zhang, *Carbohydr. Polym.*, 2017, **155**, 242–251.

18 R. K. C. Bahadur, B. Thapa and P. Xu, *Mol. Pharm.*, 2012, **9**, 2719–2729.

19 T. J. Evjen, E. A. Nilssen, S. Barnert, R. Schubert, M. Brandl and S. L. Fossheim, *Eur. J. Pharm. Sci.*, 2011, **42**, 380–386.

20 J. Olejniczak, C. J. Carling and A. Almutairi, *J. Controlled Release*, 2015, **219**, 18–30.

21 S. Ganta, H. Devalapally, A. Shahiwala and M. Amiji, *J. Controlled Release*, 2008, **126**, 187–204.

22 D. Schmaljohann, *Adv. Drug Delivery Rev.*, 2006, **58**, 1655–1670.

23 F. Q. Schafer and G. R. Buettner, *Free Radical Biol. Med.*, 2001, **30**, 1191–1212.

24 R. Cheng, F. Feng, F. Meng, C. Deng, J. Feijen and Z. Zhong, *J. Controlled Release*, 2011, **152**, 2–12.

25 D. Papahadjopoulos, T. M. Allen, A. Gabizon, E. Mayhew, K. Matthay, S. K. Huang, K. D. Lee, M. C. Woodle, D. D. Lasic and C. Redemann, *Proc. Natl. Acad. Sci. U. S. A.*, 1991, **88**, 11460–11464.

26 E. S. Lee, J. H. Kim, T. Sim, Y. S. Youn, B. J. Lee, Y. T. Oh and K. T. Oh, *J. Mater. Chem. B*, 2014, **2**, 1152–1159.

27 J. A. Grzyb and R. A. Batey, *Tetrahedron Lett.*, 2003, **44**, 7485–7488.

28 H. S. Kang, S. R. Yang, J. D. Kim, S. H. Han and I. S. Chang, *Langmuir*, 2001, **17**, 7501–7506.

29 M. Licciardi, G. Giammona, J. Du, S. P. Armes, Y. Tang and A. L. Lewis, *Polymer*, 2006, **47**, 2946–2955.

30 J. P. Salvage, S. F. Rose, G. J. Phillips, G. W. Hanlon, A. W. Lloyd, I. Y. Ma, S. P. Armes, N. C. Billingham and A. L. Lewis, *J. Controlled Release*, 2005, **104**, 259–270.